

## II. The intermediate velocity source in the $^{40}\text{Ca} + ^{40}\text{Ca}$ reaction at $E_{\text{lab}} = 35 \text{ A MeV}$

Z. Sosin<sup>1</sup>, R. Płaneta<sup>1,a</sup>, T. Ciszek<sup>1</sup>, J. Brzychczyk<sup>1</sup>, W. Gawlikowicz<sup>1</sup>, K. Grotowski<sup>1,4</sup>, S. Micek<sup>1</sup>, P. Pawłowski<sup>1</sup>, A. Wieloch<sup>1</sup>, A.J. Cole<sup>2</sup>, D. Benchekroun<sup>3</sup>, E. Bisquer<sup>3</sup>, A. Chabane<sup>2</sup>, M. Charvet<sup>2</sup>, B. Cheynis<sup>3</sup>, A. Demeyer<sup>3</sup>, P. Désesquelles<sup>2</sup>, E. Gerlic<sup>3</sup>, A. Giorni<sup>2</sup>, D. Guinet<sup>3</sup>, D. Heuer<sup>2</sup>, P. Loutesse<sup>3</sup>, L. Lebreton<sup>3</sup>, A. Llères<sup>2</sup>, M. Stern<sup>3</sup>, L. Vagneron<sup>3</sup>, and J.B. Viano<sup>2</sup>

<sup>1</sup> M. Smoluchowski Institute of Physics, Jagellonian University, Reymonta 4, 30-059 Cracow, Poland

<sup>2</sup> Institut des Sciences Nucléaires de Grenoble, IN2P3-CNRS/ Université Joseph Fourier 53, Avenue des Martyrs, F-38046 Grenoble Cedex, France

<sup>3</sup> Institut de Physique Nucléaire de Lyon, IN2P3-CNRS/ Université Claude Bernard 43, Boulevard du 11 Novembre 1918, F-69622 Villeurbanne Cedex, France

<sup>4</sup> H. Niewodniczański Institute of Nuclear Physics, Radzikowskiego 152, 31-342 Cracow, Poland

Received: 12 March 2001 / Revised version: 18 May 2001

Communicated by D. Guereau

**Abstract.** The shape of the velocity distributions of charged particles projected on the beam direction can be explained if emissions from the hot projectile-like fragment and the target-like fragment are supplemented by an emission from an intermediate velocity source located between them. The creation of this source is predicted by a two-stage reaction model where, in the second stage, some of the nucleons identified in the first stage as participants form a group of clusters located in the region between the colliding nuclei. The cluster coalescence process is governed on the average by the maximum value of entropy, although its fluctuations are also significant. The properties of the intermediate velocity source are precisely described, including the isotopic composition of the emitted particles.

**PACS.** 25.70.Gh Compound nucleus – 25.70.Lm Strongly damped collisions – 25.70.Pq Multifragment emission and correlations

### 1 Introduction

The dynamics of heavy-ion collisions in the intermediate energy domain, although they have been extensively investigated, remain insufficiently understood and explained. A characteristic feature of this region is the high multiplicity and broad mass spectrum of the emitted fragments, which can now be studied using  $4\pi$  multi-detector systems. Just as in the low-energy regime, the reactions are still reminiscent of binary collisions, and a very large fraction of the observed particles are emitted from hot projectile-like fragments (PLFs) and target-like fragments (TLFs). However, above about 10 A MeV a new class of phenomena appear in succession: fragmentation of the projectile and/or target nucleus, incomplete fusion, pre-equilibrium particle emission, and finally emission of particles with velocities intermediate between the projectile velocity and the target nucleus velocity [1,2]. It would be reasonable to suspect that this last group (and possibly also the pre-equilibrium particles) originate from a separate intermediate velocity source, IVS, located in the overlap region between the PLF

and the TLF [3–13]. A more complete list of references can be found in [8].

Similar phenomena are well known at much higher energies, where the Pauli principle is ineffective in restricting two-body energy dissipation. As a result, the overlapping portion of the colliding nuclei turns into a hot participant region (a mid-rapidity source), while the PLF and the TLF behave like spectators [14].

The situation is more complicated in the intermediate energy range, where both two-body and one-body energy dissipation may be important, as well as nuclear viscosity and surface tension. Here the reaction scenario leading to the creation of an IVS may also depend on the time scale of the reaction [11].

The existence of intermediate velocity sources was originally suggested by BUU [15] and BNV calculations [8,16]. The experimental search has been carried out by inspecting invariant velocity plots [3,4,8] or rapidity and transversal energy distributions [11,12], or by a reconstruction-subtraction procedure [10]. The so-called “aligned breakup” [7] is also highly suggestive. These observations have been done for heavy [3,4,6,7,10,13] and

<sup>a</sup> e-mail: ufplanet@cyf-kr.edu.pl

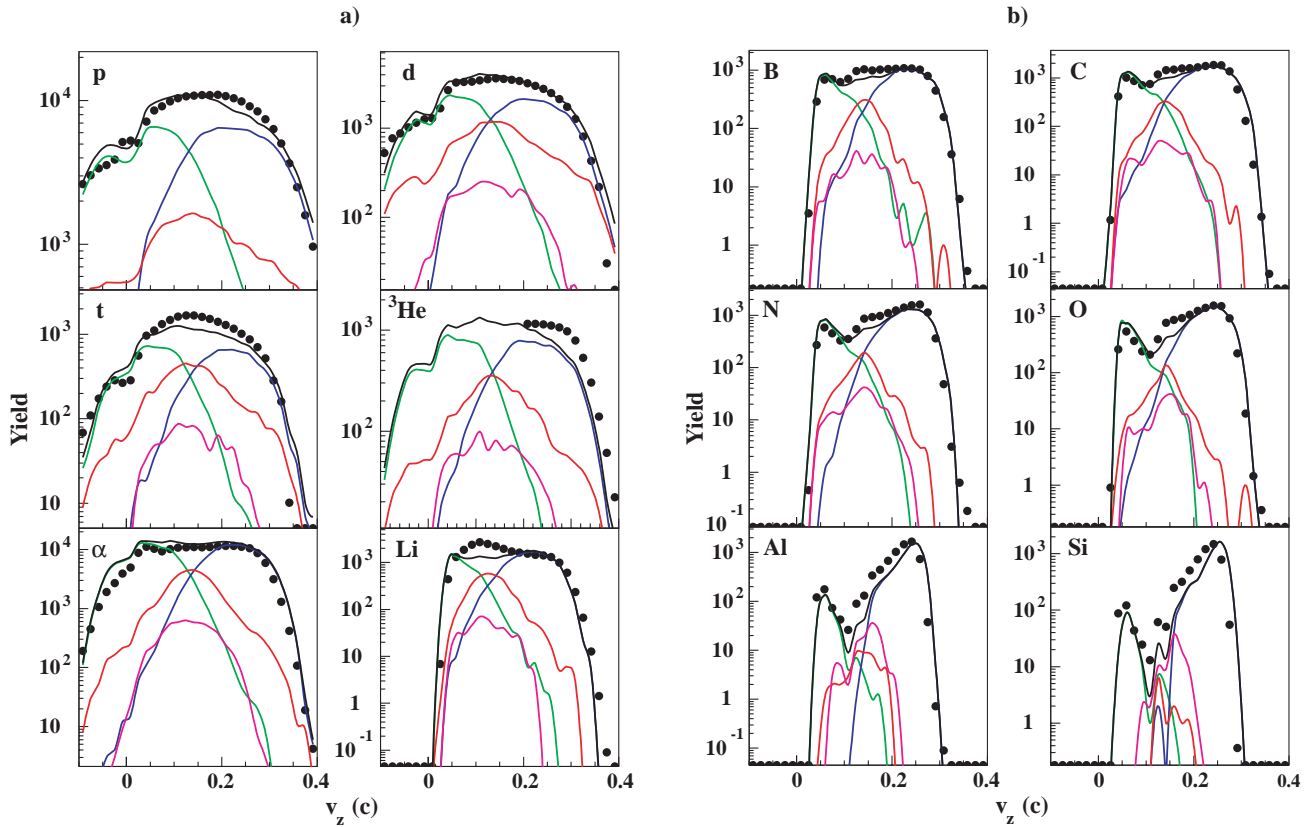


**Fig. 1.** Velocity ( $v_z$ ) distributions (LAB) projected on a direction parallel to the beam. a) Light particles; b) intermediate mass fragments; black dots: experimental data. Model predictions for IVS, PLF, and TLF sources: red, blue, and green lines, respectively. Black line: predicted total emission. Violet line: CS contribution.

medium weight [8,9,11–13] systems. The onset of mid-velocity emissions in symmetric systems has been reported close to 25 AMeV beam energy, in the vicinity of the Fermi energy [10].

According to data from several experiments [3,4,8,10], the intermediate velocity sources decay primarily by emitting intermediate mass fragments, IMFs, although the emission of light-charged particles has also been observed [3,4,10–12]. It has been suggested [3,4,10,11] that the mid-velocity matter is neutron rich (preferential emission of tritons and suppressed emission of  $^3\text{He}$  ions).

Although the existence of the IVS in heavy-ion collisions has been experimentally verified, its nature is still not well understood. For heavy systems, the emission of intermediate velocity IMFs has been explained as the dynamic fragmentation of a neck zone between the reaction partners [3,4]. This conjecture is based on 3-body relativistic Coulomb trajectory calculations. For a light system, Ar + Ni at 95 AMeV, a coalescence model coupled to the ISABEL intra-nuclear cascade code has proved to be successful in reproducing the energy and multiplicity spectra of intermediate velocity protons and light particles [9]. For peripheral and semi-central Xe + Sn collisions (25–50 AMeV), the molecular dynamics model reproduced the main characteristics of the IVS, although some differences in the amount of relative energy dissipation have been noted [10].

## 2 Experimental data and the IVS identification

The aim of the present paper is to show that some aspects of the  $^{40}\text{Ca} + ^{40}\text{Ca}$  reaction at 35 AMeV (the Fermi energy domain) are consistent with the existence of an IVS located in the center-of-mass velocity, between two Ca-like nuclei. The  $^{40}\text{Ca} + ^{40}\text{Ca}$  reaction was investigated using the Grenoble SARA facility and the AMPHORA  $4\pi$  detector system. The experimental details and mechanism of this reaction have been discussed in several papers (see [17] with references).

The creation and decay of a PLF (hot Ca-like fragment) were studied in [17] by Planeta *et al.*. The charge, mass and excitation energy distributions of the primary PLF were determined using a reconstruction procedure. De-excitation of the PLF source was also observed. The properties of the hot Ca-like source, and in particular the mass ( $A_{\text{PLF}}$ ) spectrum of the reconstructed PLF, were studied in different windows in the total transverse momentum,  $p_{\text{tr}}$ , which was used as a measure of the dissipated energy. It was noticed that although the centroid of this distribution is located close to the projectile mass in all cases, a slight shift may be observed with increasing  $p_{\text{tr}}$ . For most peripheral collisions the  $A_{\text{PLF}}$  distribution is slightly shifted towards lower values, as if part of the mass was taken up by some additional source, other than

the PLF and the TLF. For larger values of  $p_{\text{tr}}$ , the  $A_{\text{PLF}}$  distribution shifts towards slightly higher masses, which can be explained by a certain inefficiency of the PLF reconstruction procedure, resulting in contamination from another source or sources [18].

Our attempts to select the IVS source by a window located arbitrarily in the plane of the invariant velocity plot are described in [8]. As will be shown below, such procedure is only partly justified.

Similarly as in [17], for well-measured events we have imposed the event parallel momentum  $p_{\text{par}} > 8 \text{ GeV}/c$  and additionally the detection of at least one intermediate mass fragment ( $Z > 2$ ).

In order to ascertain whether or not there actually exists any such additional particle source as an IVS, the velocity distributions (LAB) of different charged particles projected on a direction parallel to the beam ( $v_z$ ) will be examined here. These are presented in fig. 1a for protons, deuterons, tritons,  $^3\text{He}$ , alpha-particles, and lithium ions and in fig. 1b for some IMFs from the  $Z = 4-14$  range. In our experiment the He isotopes were properly separated only at higher energies. Therefore, for  $^3\text{He}$  particles we present the higher velocity part of the  $v_z$  distribution. The intensity of alpha-particles is much higher than of  $^3\text{He}$  particles and therefore the  $^3\text{He}$  contamination of the low-velocity alpha-particle spectra can be neglected.

For particles with  $Z = 2-5$  the distributions exhibit some kind of plateau which is difficult to explain as a superposition of particle emission from the two most obvious sources, the PLF and the TLF. For light particles the  $v_z$  distributions resemble a Gaussian shape. Above  $Z = 5$  a deep minimum develops. The steep ridge seen at the left side of all  $v_z$  distributions results from the configuration and detection thresholds of the AMPHORA system.

## 2.1 Comparison with the Monte Carlo model

To facilitate the interpretation of the data displayed in fig. 1, we compared them to the predictions of a stochastic model proposed by Sosin (see [18] third paper in this issue) which describes a heavy-ion collision as a two-stage process. According to this model, some of the nucleons become reaction participants in the first stage by mean-field effects or by nucleon-nucleon interactions and are transferred in the second stage to the target remnant, or to the projectile remnant. Alternatively, they may form clusters located in the region between colliding Ca ions, or escape to the continuum. The nucleon transfer probabilities are governed by the state densities. The various hot fragments created in this way afterwards decay by particle emission.

Clusters and other final fragments (particles) are accelerated by Coulomb forces. Our first paper in the present issue [17] shows that such a model properly explains the creation and decay of hot Ca-like fragments.

The predictions generated by this model for the IVS, and for the PLF and TLF sources, filtered by the software replica of the AMPHORA detector, are presented by red, blue, and green lines, respectively, in fig. 1 and

in the following figures. The black line describes the total emission from all sources, while the violet line traces emissions from the composite system (CS) created in complete or incomplete fusion. In addition, the  $v_z$  distributions of deuterons, tritons and alphas are presented in fig. 2 in two  $p_{\text{tr}}$  windows. The first ( $p_{\text{tr}} < 1.5 \text{ GeV}/c$ ) represents the most peripheral collisions, while the second ( $1.5 \text{ GeV}/c < p_{\text{tr}} < 2.5 \text{ GeV}/c$ ) shows the mid-peripheral ones. In figs. 1, 2, 3 and 4 the same factor was used to normalize the model predictions to the experimental data. The level of agreement achieved is quite acceptable.

It can be seen that all particles are emitted from the hot PLF, the hot TLF, and the intermediate velocity source. The CS emission predicted by the model is small (fig. 1), corresponding to several dozen millibarns, consistent with the experimental supposition (see *e.g.* [14]). It is concentrated in the region of more central collisions (see [18]) and outside the logarithmic scale of fig. 2. For heavier fragments the IVS contribution rapidly decreases while the CS emission becomes more significant.

The model calculations have been repeated with a condition excluding the formation of clusters. It is clear (see fig. 5) that with this restriction the model is no longer able to describe the experimental data. The exclusion of clusters results in the over-production of protons emit-

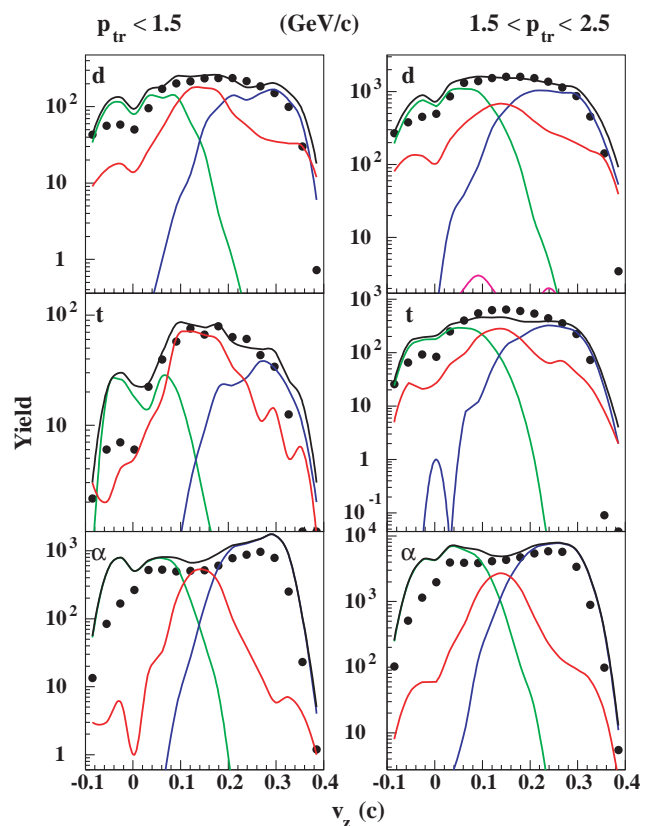


**Fig. 2.** Velocity ( $v_z$ ) distributions (LAB) of deuterons, tritons, and alphas. Model predictions and experimental points. The key for the lines is the same as in fig. 1. The  $p_{\text{tr}}$  windows: left:  $p_{\text{tr}} < 1.5 \text{ GeV}/c$ ; right:  $1.5 \text{ GeV}/c < p_{\text{tr}} < 2.5 \text{ GeV}/c$ .

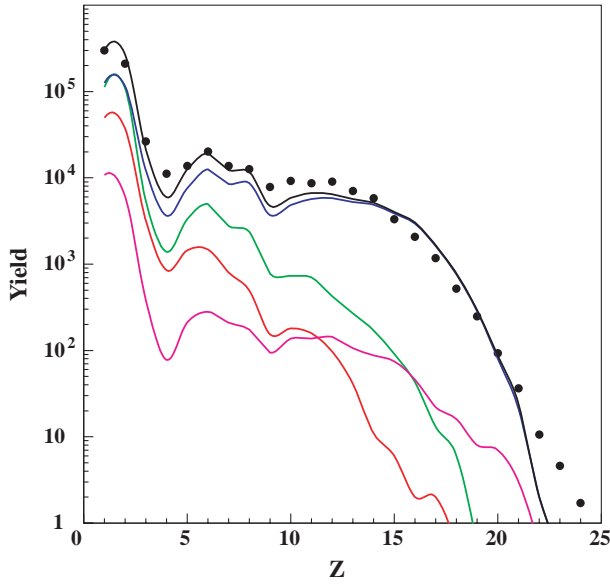


**Fig. 3.**  $Z$  distributions of particles emitted by the IVS and by the PLF and TLF sources. Model predictions and experimental points. The key for the lines is the same as in fig. 1.

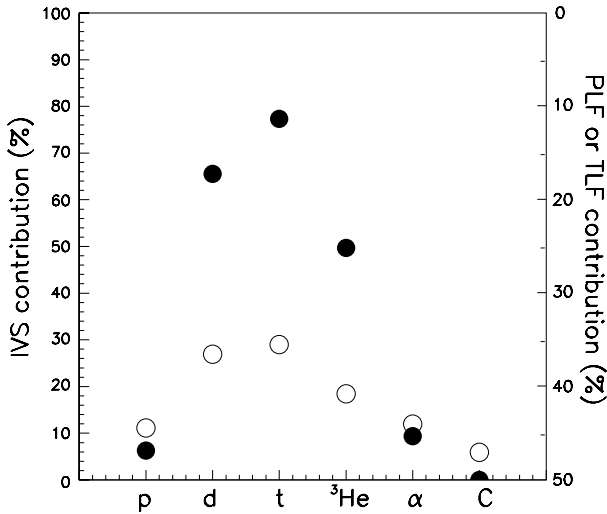


**Fig. 4.** Relative contribution of the IVS source in the emission of different ejectiles (percent of the total emission); model prediction with no experimental limitations. The PLF and TLF contributions are shown on the right vertical axis. Black dots:  $L > 200\hbar$  (peripheral collisions). Open circles: full range of  $L$  values.

ted from the mid-velocity region. For tritons, alphas and heavier particles two maxima appeared in the model predictions, which is not consistent with experimental data.

The relative intensities of the different ejectiles emitted by the IVS and by the PLF and TLF sources, as predicted by the model and seen by the AMPHORA detector, are presented in table 1. Protons, alphas and carbon ions are primarily emitted from the PLF and TLF sources (83, 84, and 89%, respectively). The IVS emission of tritons, deuterons and  $^3\text{He}$  particles is relatively stronger. We can see, however, that in the case of peripheral collisions, tri-

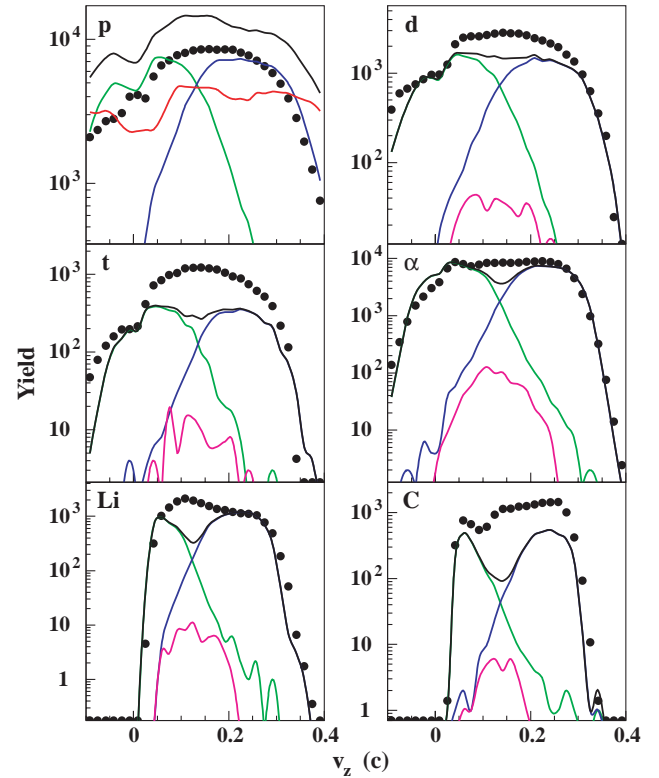


**Fig. 5.** Velocity ( $v_z$ ) distributions (LAB) of protons, deuterons, tritons, alphas, lithium, and carbon ions. Experimental points and model predictions without clusters. The key for the lines is the same as in fig. 1.

tons, deuterons and also but to a lesser extent  $^3\text{He}$ , are more preferentially emitted from the intermediate velocity source (55, 38 and 24%, respectively).

Figure 3 presents the charge ( $Z$ ) distributions of the particles emitted by the PLF, TLF, and IVS sources, as predicted by the model and seen by the AMPHORA detector. The emission of light particles prevails for all three sources. The intensity of the IMF emission decreases with the  $Z$  value. This decrease is faster for the IVS particles, and does not indicate the quasi-plateau observed for the total PLF emission between  $Z = 4$  and  $Z = 12$ .

**Table 1.** Relative intensities (percent) of different ejectiles emitted by the PLF, TLF, IVS and CS sources, as seen by the AMPHORA system (model predictions).

	all $p_{tr}$				$p_{tr} < 1.5 \text{ GeV}/c$		
	PLF	TLF	IVS	CS	PLF	TLF	IVS
Protons	44.3	38.3	13.6	3.8	48.2	44.8	7.0
Deuterons	37.3	34.5	23.7	4.5	32.8	29.1	38.1
Tritons	35.2	34.5	25.5	4.8	26.4	18.9	54.7
$^3\text{He}$	39.0	38.1	17.7	5.2	49.2	26.6	24.1
Alphas	43.5	40.9	13.4	2.2	54.5	31.3	14.2
Carbon ions	64.4	24.9	8.7	1.9	92.7	3.1	4.2

**Table 2.** Contribution (percent) of different ejectiles emitted by the IVS and by the PLF and TLF sources, observed in the IVS window (model predictions).

	all $p_{\text{tr}}$			$p_{\text{tr}} < 1.5 \text{ GeV}/c$		
	IVS	PLF	TLF	IVS	PLF	TLF
Deuterons	21	39	40	43	25	32
Tritons	32	34	34	67	19	14
Alphas	28	36	35	53	23	24
Lithium ions	35	36	28	67	23	10
Beryllium ions	37	46	17	62	38	0
Boron ions	39	37	24	67	24	9
Carbon ions	27	46	27	36	54	10
Nitrogen ions	28	53	19	25	69	6
Oxygen ions	23	61	16	8	92	0

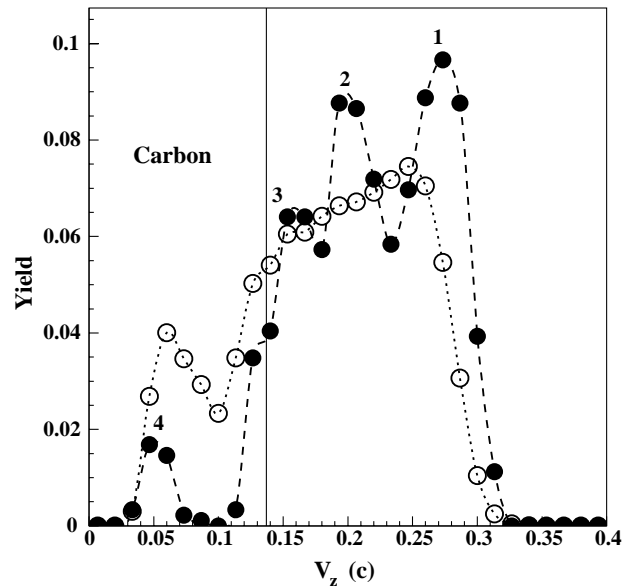
### 3 Competition of different sources without the AMPHORA filter limitations

The reaction picture presented in sect. 2 for the experimental data and for the model predictions is distorted by the AMPHORA detector (filter) and by the conditions imposed for the well-defined events. Figure 4 presents the relative contribution of the IVS source in emission of different ejectiles, predicted by the model with no experimental limitations. The IVS contribution is given in percent of the total emission. For the symmetric  $^{40}\text{Ca} + ^{40}\text{Ca}$  reaction the PLF and TLF contributions are equal, and are shown on the right vertical axis. We neglect here the small CS contribution. Black dots represent the emission for the entrance channel angular momentum  $L > 200\hbar$  (peripheral collisions), open circles the emission in the full range of  $L$  values. As seen from fig. 4, in peripheral collisions tritons, deuterons and  $^3\text{He}$  particles are preferentially emitted by the IVS (77, 65 and 49%, respectively) and the IVS emission of neutron-rich tritons and deuterons is slightly enhanced.

Light particles emitted by the IVS belong to two categories: i) cold deuterons, tritons,  $^3\text{He}$ , alpha-particles, and heavier fragments born in the coalescence process and not able to decay by the particle emission; ii) particles evaporated from the excited IVS clusters. The contribution of deuterons, tritons,  $^3\text{He}$ , alphas, lithium and carbon ions, belonging to the first category is respectively: 66, 62, 51, 25, 26 and 4%.

### 4 Selection of the IVS emission by a “window”

In some experiments [3,4,8], the IVS was selected by a window located, more or less arbitrarily, in the plane of the invariant velocity plot. Such a window, a circle centered at the CM velocity ( $0.13c$ , LAB) with a radius of  $0.05c$ , was used in our previous work [8] to select IMFs coming from the IVS. It would be appropriate to ask how large the contribution of particles from the PLF and TLF sources lies inside such a window. The model calculations show that

**Fig. 6.** Velocity ( $v_z$ ) distribution (LAB) of carbon ions (experiment). Black dots:  $p_{\text{tr}} < 1.2 \text{ GeV}/c$ . Open circles: all  $p_{\text{tr}}$  values.

the PLF and TLF contribution (contamination) is considerable (in the case of protons it comes to 90%). Table 2 summarizes this problem in detail for different ejectiles, from deuterons up to oxygen ions. Roughly speaking, the PLF and TLF contamination inside the IVS window decreases slightly with the observed ejectile charge. For the full range of impact parameters (with no  $p_{\text{tr}}$  limitations) the contamination drops from about 70% for tritons and alphas to the level of about 61% for boron ions. The situation is better for peripheral collisions, where from tritons up to boron ions the contamination is roughly twice smaller. As table 2 makes clear, the levels of the PLF and TLF contamination begin to increase slowly above  $Z = 5$ , where the intermediate velocity source is unable to compete (in intensity) with the PLF and TLF sources (see fig. 3).

### 5 Production of fragments for most peripheral collisions

Peripheral collisions produce the PLF and TLF fragments with very little excitation energy, but some of them with a large angular momentum. Such fragments emit only a few light particles, but can undergo fission induced by angular momentum [19]. If peripheral collisions are enhanced by the small value of  $p_{\text{tr}}$ , the fission fragments should be aligned close to the beam direction. Consequently, the projected velocity distribution should present two PLF maxima and two TLF maxima, respectively. The IVS particles should produce one maximum centered at the CM velocity. Figure 6 presents such a picture for the carbon ejectiles with  $p_{\text{tr}} < 1.2 \text{ GeV}/c$  (black dots). Peaks (1) and (2) belong to PLF fission, while TLF fission is represented by peak (4). The second TLF peak, located in the re-

gion of negative CM velocities, is not observed because of the detection thresholds. The IVS emission is represented by peak (3). In order to resolve peaks (1)-(4) properly, a rather low value for  $p_{tr}$  must be assumed. For comparison, open circles present the same picture but without restriction for the  $p_{tr}$  values. The well-resolved peaks (solid points) shown in fig. 4 require a rather large statistics (about  $2 \times 10^8$  events in our experiment). It is so because of the  $p_{tr}$  restrictions and due to the fact that the carbon ejectiles are not preferentially emitted by the intermediate velocity source.

## 6 Summary and conclusions

It has been demonstrated that in the case of the  $^{40}\text{Ca} + ^{40}\text{Ca}$  reaction at 35 A MeV (the Fermi energy region), the particle velocity distributions projected on the beam direction are properly explained by emission of particles from three sources, the PLF, TLF and IVS. The presence of the intermediate velocity source has a major impact on the shape of these distributions. For peripheral collisions, the emission from this IVS of some intermediate mass fragments and light particles as well may also be observed in a window located in the invariant velocity plane. However, the contamination from other particle sources is significant or even dominant, and should be taken into account.

The origin and properties of this intermediate velocity source are properly described by the stochastic coalescence process of nucleons liberated in the collision of Ca ions. The reaction scenario, and in particular the coalescence process, are governed on the average by the maximum value of entropy. The created intermediate velocity source can be considered as a multi-component gas of nucleons and clusters of different degree of excitation. This system separates afterwards under the influence of Coulomb forces.

The yield of particles emitted from the IVS decreases with the increasing value of particle  $Z$ . About 94% of them are light particles.

In peripheral collisions tritons, deuterons and, to a lesser extent,  $^3\text{He}$  particles are preferentially emitted from the IVS. The dominance of the neutron-rich triton emission over the neutron-poor  $^3\text{He}$  one is preserved and intensified also for more central collisions. This observation is consistent with earlier reported ones [3,4,10,11], and various explanations have been discussed, such as a relation between the  $N/Z$  ratio and the source size [4], an analogy to the emission of particles accompanying fission [4], the problem of the charge-to-mass equilibration [4,20,21], and even the isospin dependence of the nuclear matter

equation of state (see [21] with references). To date no final conclusion has been reached. Our model is able to reproduce this triton, deuteron and  $^3\text{He}$  anomaly. It describes the heavy-ion collision as a stochastic coalescence process governed by the state densities and by the distribution of  $Q$ -values along the chain of stochastic steps. This process and the decay of the excited clusters (fragments) created in this way are decisive for the reaction picture.

In the evaporation process, the intensity ratio of the emitted tritons and  $^3\text{He}$  particles increases with the decreasing size of the evaporating source (see the GEMINI code [22]). This dependence was suggested in [4] as explanation of the triton- $^3\text{He}$  anomaly. It should be mentioned however, that the triton over the  $^3\text{He}$  dominance, predicted by our model and observed in our experimental data, can be only partly related to this effect. Due to the low density of states, over 50% of light particles are born as the cold ones.

This work was supported by the Scientific Research Commission of Poland (KBN Grant PB 1188/P03/98/14) and the M.Sklodowska-Curie Fund (MEN/DOE- 97-318). Calculations for this work were partly performed using facilities of the Cracow Academic Computing Center, CYFRONET (KBN Grant No. S2000/UJ/157/1998).

## References

1. L. Stuttgé et al., Nucl. Phys. A **539**, 511 (1992).
2. B. Lott et al., Phys. Rev. Lett. **68**, 3141 (1992).
3. J. Töke et al., Nucl. Phys. A **583**, 519 (1995).
4. J.F. Dempsey et al., Phys. Rev. C **54**, 1710 (1996).
5. Y. Larochelle et al., Phys. Rev. C **55**, 1869 (1997).
6. J. Lukasik et al., Phys. Rev. C **55**, 1906 (1997).
7. F. Bocage et al., Nucl. Phys. A **676**, 391 (2000).
8. P. Pawłowski et al., Phys. Rev. C **57**, 1771 (1998).
9. P. Pawłowski et al., Eur. Phys. J. A **9**, 371 (2000).
10. E. Plagnol et al., Phys. Rev. C **61**, 014606 (2000).
11. T. Lefort et al., Nucl. Phys. A **662**, 397 (2000).
12. D. Dore et al., Phys. Lett. B **491**, 15 (2000).
13. V. Métivier et al., Nucl. Phys. A **672**, 357 (2000).
14. J. Péter et al., Nucl. Phys. A **593**, 95 (1995).
15. L.G. Sobotka, Phys. Rev. C **50**, R1272 (1994).
16. M. Colonna et al., Nucl. Phys. A **583**, 525c (1995).
17. R. Planeta et al., this issue, p. 297.
18. Z. Sosin, this issue, p. 311.
19. K. Grotowski et al., Phys. Rev. C **30**, 1214 (1984); K. Grotowski, R. Planeta, M. Blann, T. Komoto, Phys. Rev. C **39**, 1320 (1989).
20. R. Planeta et al., Phys. Rev. C **38**, 195 (1988).
21. L.G. Sobotka, Acta Phys. Pol. B **31**, 1535 (2000).
22. R.J. Charity et al., Nucl. Phys. A **483**, 371 (1988).